Nonequilibrium effects in model reactive systems: The role of species temperatures

Duncan G. Napier and Bernie D. Shizgal
Department of Chemistry, University of British Columbia, Vancouver, British Columbia, Canada V6T 1Z1
(Received 13 April 1995)

The nonequilibrium effects for a model reactive system, $A + B \rightarrow$ products, that arise from the perturbation of the distribution function from the Maxwellian are studied. The main objective is the calculation of the fractional decrease of the nonequilibrium rate coefficient from the equilibrium value. This effect is examined with the Chapman-Enskog method of solution of the Boltzmann equation which treats the reactive processes as a weak perturbation. The approach is referred to as weak nonequilibrium. The reactive process causes the temperatures of the two species to differ from the system temperature and this effect can play an important role in the determination of the departure of the rate coefficient from the equilibrium value. A second method is an extension of the Chapman-Enskog approach and involves the expansion of the distribution functions about Maxwellians at different temperatures and is referred to as strong nonequilibrium (SNE). A third approach is a modification of SNE and is referred to as modified strong nonequilibrium. The three methods are described and departures of the rate coefficients from their equilibrium values are computed for each case and compared, along with an explicitly time-dependent solution of the Boltzmann equation.

PACS number(s): 05.20.Dd, 51.10.+y, 47.70.Nd

I. INTRODUCTION

The departure from equilibrium of chemically reactive systems has been of concern for over four decades [1–10] and continues to be of considerable interest as a fundamental kinetic theory problem as well as of practical importance. These nonequilibrium effects are associated with the reentry of space vehicles in the terrestrial atmosphere [11], plasma processing of materials [12], molecular transport coupled to chemical nonequilibrium [13], and other systems. The main objective is the theoretical description of physical situations that may be far from equilibrium. The usual approach to the description of systems close to equilibrium is based on the Chapman-Enskog solution for neutral and ionized systems [14,15]. This method is known to be invalid for strongly nonequilibrium systems for which the required separation of length and time scales is not obtained [16–20]. Several groups have considered the description of transport for such systems far from equilibrium; in particular, nonlocal heat transport in plasmas [16], hypersonic flows [17], diffusive flows [18,19], as well as astrophysical applications [20]. For spatially inhomogenous systems, the Chapman-Enskog method is valid when the mean free path of the constituents is much less than the typical length scale [14,15]. For reactive systems, a Chapman-Enskog method is applicable when the elastic time scale is much less than the reactive time scale [8]. Kogan [21] and Alexeev and co-workers [22–24] have considered extensions of the Chapman-Enskog method to chemically reactive systems far removed from equilibrium. Aleexev has referred to this method as the generalized Chapman-Enskog method. The development of techniques to describe such systems is an important endeavor. The present paper, although restricted to a spatially homogeneous reactive model system, is a detailed study of alternatives to the Chapman-Enskog method in situations similar to the above when the required separation of time scales does not exist. This work is also motivated by the general methods of solution of the Boltzmann equation introduced by Pascal and Brun [13] in their study of transport processes in molecular systems.

The main purpose of this paper is to reexamine the nonequilibrium effects associated with a simple reactive system of the type

$$A + B \rightarrow \text{products},$$

where the reactive process perturbs the distribution functions of both species from the equilibrium Maxwellian distributions and the rate coefficient differs from the equilibrium rate coefficient. If $k^{(0)}$ and k are the equilibrium and nonequilibrium rate coefficients, respectively, the fractional decrease of the nonequilibrium rate coefficient from the equilibrium rate coefficient defined by,

$$\eta = [k - k^{(0)}]/k^{(0)} \tag{1}$$

is the main objective of these studies. The determination of these nonequilibrium effects in a model system based on the Chapman-Enskog method has been studied in detail in previous papers [5–8]. Additional references to earlier papers are to be found in the papers referenced. The distribution functions are expressed in terms of Maxwellians at the *same temperature* plus a small correction that arises because of the reactive process. The departure of the distribution functions from Maxwellians is then determined with a Chapman-Enskog type approach [14] that has been described at length in previous papers [5–7]. We briefly review this approach in Sec. II of the paper. This approach has been referred

to as weak nonequilibrium (WNE) by Pascal and Brun [13] in their recent study of transport processes in molecular systems. In this case the distribution function for the molecular system is expanded about a single temperature even though the translational and vibrational temperatures may differ. The different species temperatures in the present paper are somewhat analogous to different translational and vibrational temperatures in molecular systems. We show that the WNE method is valid provided that the elastic cross sections for *A-A*, *B-B*, and *A-B* collisions are the same order of magnitude and much larger than the reactive collision cross section. The usual Chapman-Enskog approach to this problem [1–7] is based on the treatment of the reactive process as a small perturbation on the elastic collision processes that restore the system to equilibrium. This is equivalent to the recognition that reactive cross sections are typically much smaller than elastic cross sections.

In Sec. III, we consider a situation for which the elastic cross sections for *A-A* and *B-B* collisions are similar and much larger than the cross sections for elastic *A-B* and reactive *A-B* collisions. The different magnitudes of these cross sections yield different time scales and are used to obtain Chapman-Enskog-like solutions. For this situation, distribution functions are expanded about Maxwellians at *different temperatures* and the departure from equilibrium of these local Maxwellians is calculated. Pascal and Brun refer to this approach as strong nonequilibrium (SNE) and in their application expand the distribution function about equilibrium Boltzmann distributions at different translational and vibrational temperatures. There are many different physical situations far from equilibrium for which the coupling of different species is weak and thus they are characterized with distribution functions at different temperatures. This is most notable in plasma systems where electron-ion and electron-neutral collision rates are relatively small and electron temperatures can be considerably different from ion and/or neutral temperatures. The transport theory of plasmas [27] takes this feature into account. These phenomena are evident in the ionosphere where departures from equilibrium occur owing to the influence of electromagnetic fields on charged particles and also because of chemical reactions [25–27]. The transport theory of the drift of ions in an electric field involves the specification of different temperatures for the ion velocity distributions for velocities parallel and perpendicular to the electric field [28]. For chemically reactive systems similar to the model systems considered in this paper, Cukrowski and co-workers [9,10] have discussed at length the effects of different species temperatures.

In Sec. IV, we present a modification of the SNE approach and introduce a modified strong nonequilibrium (MSNE). This was discussed by Pascal and Brun since their results with SNE do not coincide with WNE when the vibrational and translational temperatures coincide. With the MSNE formalism, previously referred to as the generalized Chapman-Enskog method [13,21–24], the results for SNE coincide with WNE in the limit of equal translational and vibrational temperatures. We apply this MSNE approach to the model reactive systems of this paper and compare the results with WNE and SNE. In order to understand the range of validity of the three methods, we consider a rigorous time-dependent solution of the Boltzmann equations and investigate the establishment of the steady states assumed in the WNE, SNE, and MSNE approaches. A comparison of the three formalisms is then discussed and compared with the explicit time-dependent results in Secs. VI and VII.

II. THE CHAPMAN-ENSKOG APPROACH—WEAK NONEQUILIBRIUM (WNE)

The methodology for the study of the nonequilibrium effects in the reactive process has been presented in earlier papers [5–7]. We present here a brief summary of the approach and include most of the equations for completeness so that we can compare with the other formalisms in Secs. III and IV. The distribution functions for species $\gamma = 1$ and 2, for this spatially homogeneous system in the absence of external forces, are assumed to be given by two coupled Boltzmann equations of the form

$$\frac{\partial f_1}{\partial t} = \frac{1}{\epsilon}\left[\int\int [f_1' f' - f_1 f]\sigma_{11} g d\Omega d\mathbf{c} + \int\int [f_1' f_2' - f_1 f_2]\sigma_{12} g d\Omega d\mathbf{c}_2\right] - \int\int f_1 f_2 \sigma^* g d\Omega d\mathbf{c}_2, \tag{2}$$

$$\frac{\partial f_2}{\partial t} = \frac{1}{\epsilon}\left[\int\int [f_2' f' - f_2 f]\sigma_{22} g d\Omega d\mathbf{c} + \int\int [f_1' f_2' - f_1 f_2]\sigma_{12} g d\Omega d\mathbf{c}_1\right] - \int\int f_1 f_2 \sigma^* g d\Omega d\mathbf{c}_1, \tag{3}$$

where $\sigma_{\gamma\eta}$ and σ^* are the elastic and reactive cross sections, respectively. The first collision operators on the left-hand side (LHS) of Eqs. (2) and (3) are the *self*-collision terms for *A-A* and *B-B* elastic collisions. The second and third collision operators take account of *A-B* collisions and couple the two equations. The *A-A* and *B-B* elastic collisions will be referred to as 1-1 collisions while *A-B* elastic collisions will be referred to as 1-2 elastic collisions to keep them consistent with the notation in Eqs. (2) and (3). The other terms and the notation used have been defined in the previous papers [5–7]. These time-dependent equations are solved with the assumption that the reactive cross sections are small relative to the elastic cross sections. The parameter $\epsilon \approx \sigma/\sigma^*$ has been inserted into the Boltzmann equations to take this ordering of collision terms into account. We thus set

$$f_\gamma = f_\gamma^{(0)}[1 + \epsilon\psi_\gamma] \tag{4}$$

and the equations of order $1/\epsilon$ obtained with Eq. (4) in Eqs. (2) and (3) determine that the zero order distribution functions,

$$f_\gamma^{(0)} = n_\gamma(t)[m_\gamma/2\pi kT(t)]^{3/2}\exp[-m_\gamma c_\gamma^2/2kT(t)] ,$$

are the Maxwellians characterized by time-dependent number densities, $n_\gamma(t)$, and the *single* temperature, $T(t)$. The term ψ_γ is the perturbation from Maxwellian.

The Chapman-Enskog approach [14] involves the assumption that a steady state occurs in a time short on the reactive time scale and that the time dependence is implicit through the variation with time of the number densities and the temperature. With this assumption we have that to lowest order,

$$\frac{\partial f_\gamma}{\partial t} = \frac{\partial f_\gamma^{(0)}}{\partial n_\gamma}\left(\frac{dn_\gamma}{dt}\right)^{(0)} + \frac{\partial f_\gamma^{(0)}}{\partial T}\left(\frac{dT}{dt}\right)^{(0)} , \tag{5}$$

where the variation with time is determined from the Boltzmann equations and we have that

$$\left(\frac{dn_1}{dt}\right)^{(0)} = \left(\frac{dn_2}{dt}\right)^{(0)} = -\int\int\int f_1^{(0)} f_2^{(0)} \sigma^* g d\Omega d\mathbf{c}_1 d\mathbf{c}_2, \tag{6}$$

$$\left(\frac{dT}{dt}\right)^{(0)} = \frac{2T}{3n}\int\int\int f_1^{(0)} f_2^{(0)}\left[3 - \frac{m_1 c_1^2}{2kT} - \frac{m_2 c_2^2}{2kT}\right]\sigma^* g d\Omega d\mathbf{c}_1 d\mathbf{c}_2. \tag{7}$$

With the substitution of Eq. (4) into the Boltzmann equations, Eqs. (2) and (3), and use of Eqs. (5)–(7), we find the Chapman-Enskog equations for the perturbations ψ_γ, by equating terms of zero order in ϵ,

$$\int\int f_1^{(0)} f^{(0)}[\psi_1' + \psi' - \psi_1 - \psi]\sigma_{11} g d\Omega d\mathbf{c} + \int\int f_1^{(0)} f_2^{(0)}[\psi_1' - \psi_1]\sigma_{12} g d\Omega d\mathbf{c}_2 + \int\int f_1^{(0)} f_2^{(0)}[\psi_2' - \psi_2]\sigma_{12} g d\Omega d\mathbf{c}_2 = f_1^{(0)} H_1(c_1) , \tag{8}$$

$$\int\int f_2^{(0)} f^{(0)}[\psi_2' + \psi' - \psi_2 - \psi]\sigma_{22} g d\Omega d\mathbf{c} + \int\int f_1^{(0)} f_2^{(0)}[\psi_2' - \psi_2]\sigma_{12} g d\Omega d\mathbf{c}_1 + \int\int f_1^{(0)} f_2^{(0)}[\psi_1' - \psi_1]\sigma_{12} g d\Omega d\mathbf{c}_1 = f_2^{(0)} H_2(c_2) , \tag{9}$$

where the inhomogeneous terms are defined by

$$H_\gamma(c_\gamma) = \left[-\frac{1}{n_\gamma}\left(\frac{dn_\gamma}{dt}\right)^{(0)} - \frac{1}{T}\left(\tfrac{3}{2} - x_\gamma^2\right)\left(\frac{dT}{dt}\right)^{(0)} + \int f_\eta^{(0)}\sigma^* g d\Omega d\mathbf{c}_\eta\right], \quad \gamma = 1,2 , \tag{10}$$

where $x_\gamma^2 = m_\gamma c_\gamma^2/2kT$.

The solution of these coupled linear integral equations is obtained with the expansion of the unknown functions ψ_γ in Sonine (Laguerre) polynomials, $S_\gamma^{(i)}(x_\gamma^2)$, defined in previous papers [5,6]. With the expansions

$$\psi_\gamma(x_\gamma) = \sum_{j=1}^{N} a_j^{(\gamma)} S_\gamma^{(j)}(x_\gamma^2) \tag{11}$$

we get the set of algebraic equations for the coefficients $a_j^{(\gamma)}$ given by

$$\sum_{j=1}^{N}\left[\left(n_1^2[S_1^{(i)}, S_1^{(j)}] + n_1 n_2\{S_1^{(i)}, S_1^{(j)}\}\right)a_j^{(1)} + n_1 n_2\{S_1^{(i)}, S_2^{(j)}\}a_j^{(2)}\right] = n_1 n_2 \alpha_i^{(1)} \tag{12}$$

and

$$\sum_{j=1}^{N}\left[\left(n_2^2[S_2^{(i)}, S_2^{(j)}] + n_1 n_2\{S_2^{(i)}, S_2^{(j)}\}\right)a_j^{(2)} + n_1 n_2\{S_2^{(i)}, S_1^{(j)}\}a_j^{(1)}\right] = n_1 n_2 \alpha_i^{(2)}, \tag{13}$$

where the bracket matrix elements $[S_\gamma^{(i)}, S_\gamma^{(j)}]$, the brace matrix elements $\{S_\gamma^{(i)}, S_\eta^{(j)}\}$, and the coefficients $\alpha_i^{(\gamma)}$ are defined by Eqs. (29)–(33) of [6]. The density is defined in terms of $f_\gamma^{(0)}$, that is,

$$n_\gamma = \int f_\gamma^{(0)} d\mathbf{c}_\gamma , \tag{14}$$

so that $\int f_\gamma^{(0)}\psi_\gamma d\mathbf{c}_\gamma = 0$ and hence $a_0^{(0)} = 0$. An important aspect of this WNE approach is that the *single* temperature is defined by

$$\tfrac{3}{2}nkT = \int f_1^{(0)} \tfrac{1}{2} m_1 c_1^2 d\mathbf{c}_1 + \int f_2^{(0)} \tfrac{1}{2} m_2 c_2^2 d\mathbf{c}_2 , \tag{15}$$

where $n = n_1 + n_2$. As a consequence of this definition we have that

$$\int f_1^{(0)} m_1 c_1^2 \psi_1 d\mathbf{c}_1 + \int f_2^{(0)} m_2 c_2^2 \psi_2 d\mathbf{c}_2 = 0 \qquad (16)$$

and hence

$$n_1 a_1^{(1)} + n_2 a_1^{(2)} = 0. \qquad (17)$$

Consistent with this definition of the temperature is that the two equations in Eqs. (12) and (13) with $i = 1$ are the negative of one another; their sum being equal to zero is a reflection of conservation of energy when both species are taken into account. Consequently, the set of equations that are solved is the set with Eq. (17) replacing either of the two equations with $i = 1$ in Eqs. (12) and (13).

The solution of Eqs. (12) and (13) together with Eq. (17) as discussed above yields the expansion coefficients and the fractional decrease in the equilibrium rate of reaction and is given by

$$\eta^{\mathrm{WNE}} = -\sum_{\gamma=1}^{2}\sum_{i=1}^{N} a_i^{(\gamma)} A_i^{(\gamma)}/A_0 \ , \qquad (18)$$

where the $A_i^{(\gamma)}$ integrals are defined by

$$A_i^{(\gamma)} = \int\int\int f_1^{(0)} f_2^{(0)} S_\gamma^{(i)} \sigma^* g d\Omega d\mathbf{c}_1 d\mathbf{c}_2 \ . \qquad (19)$$

Numerical results have generally been considered for elastic hard sphere cross sections, $\sigma_{\gamma\eta} = d_{\gamma\eta}^2/4$, and the line-of-centers reactive total collision cross section model, $\sigma_{\mathrm{tot}}^* = \pi d_r^2(1 - E^*/E)$ for $E \geq E^*$, and zero otherwise, where E is the relative translational energy. The parameter E^* corresponds to the activation energy. The details for the evaluation of collision matrix elements and other quantities in Eqs. (12) and (13) can be found in [5] and [6]. Detailed results for the correction to the rate of reaction for this model system were reported in the previous papers [5–7]. In this paper, we emphasize the role of different species temperatures on the nonequilibrium effects.

The calculation of the mean energy of each species yields the definition of species temperatures, T_γ, which are given explicitly by

$$T_\gamma = T[1 - a_1^{(\gamma)}]. \qquad (20)$$

These have been referred to as the Shizgal-Karplus temperatures [9,10]. In this WNE approach, the temperatures of both species are perturbed strongly from their value, T, for the equilibrium state. The values of $a_1^{(\gamma)}$ for which the WNE is valid are expected to be small as demonstrated in Sec. IV. However, this temperature effect can vanish for specific choices of the system parameters for which $\alpha_1^{(\gamma)} = 0$, even for a strong reaction. The moments $\alpha_1^{(1)}$ and $\alpha_1^{(2)}$ of the inhomogeneous terms in the Boltzmann equations [6] involve considerations of energy balance and can be shown to be proportional to $(\frac{m_1 n_1}{m_2 n_2} - 1)$ and $(\frac{m_2 n_2}{m_1 n_1} - 1)$, respectively, and hence vanish for $\frac{m_2 n_2}{m_1 n_1} = 1$. The behavior of the nonequilibrium correction, η, versus the system parameters (m_γ, n_γ, and E^*/kT) is determined in a large part by the departures of T_γ from T, for $\frac{m_2 n_2}{m_1 n_1} \neq 1$.

It is useful to recognize that the expansion of a local Maxwellian at temperatures T_γ can be expressed as the Maxwellian at temperature T in terms of Sonine polynomials in the form

$$F_\gamma^{(0)}(T_\gamma) = f_\gamma^{(0)}(T)\left[1 + \sum_{i=1}^{N} S_\gamma^{(i)}(T)\left(\frac{T - T_\gamma}{T}\right)^i\right]. \qquad (21)$$

The ratio $F_\gamma^{(0)}(T_\gamma)/f_\gamma^{(0)}(T)$ is the generating function for the Sonine polynomials employed to evaluate the collision matrix elements [6,7,29]. Using Eq. (20), it can be shown that the coefficient $\left(\frac{T-T_\gamma}{T}\right)$ is just the first term $a_1^{(\gamma)}$ of the expansion in Eq. (11).

III. STRONG NONEQUILIBRIUM (SNE)

Since it appears that the species temperatures can play an important role, it is useful to consider the expansion of the distribution functions about local Maxwellians characterized by densities n_γ and *different* species temperatures, T_γ, that remain to be specified. This is equivalent to the assumption that the rate of collisions between unlike species is very slow relative to the self-collision rate. This is an approach that is considered in plasma systems [27], in ionospheric applications [25,26], and is also employed in the determination of mobility of ions in neutral gases [28]. The Boltzmann equations, Eqs. (2) and (3), are rewritten in the form

$$\frac{\partial f_1}{\partial t} = \frac{1}{\epsilon}\left[\int\int [f_1' f' - f_1 f]\sigma_{11} g d\Omega d\mathbf{c}\right] + \int\int [f_1' f_2' - f_1 f_2]\sigma_{12} g d\Omega d\mathbf{c}_2 - \int\int f_1 f_2 \sigma^* g d\Omega d\mathbf{c}_2 \ , \qquad (22)$$

$$\frac{\partial f_2}{\partial t} = \frac{1}{\epsilon}\left[\int\int [f_2' f' - f_2 f]\sigma_{22} g d\Omega d\mathbf{c}\right] + \int\int [f_1' f_2' - f_1 f_2]\sigma_{12} g d\Omega d\mathbf{c}_1 - \int\int f_1 f_2 \sigma^* g d\Omega d\mathbf{c}_1 \ , \qquad (23)$$

where the term in $1/\epsilon$ multiplies only the self-collision integral term. The collision term between unlike species is considered to be much smaller than the like species collision term. The exchange of energy between components is slow owing to a small $\sigma_{\gamma\eta}$ cross section or a disparate mass ratio.

The distribution function is now written in the form

$$f_\gamma = F_\gamma^{(0)}[1 + \epsilon\phi_\gamma] \ , \qquad (24)$$

where $F_\gamma^{(0)} = n_\gamma(t)[m_\gamma/2\pi k T_\gamma(t)]^{3/2} \exp[-m_\gamma c^2/2kT_\gamma(t)]$ is the local Maxwellian, the solution to the equation of order $1/\epsilon$ that results with the substitution of Eq. (24)

into Eqs. (22) and (23). The local Maxwellians are characterized by different temperatures, $T_\gamma(t)$. The time dependence of the species densities and temperatures to lowest order is given by

$$\left(\frac{dn_1}{dt}\right)^{(0)} = \left(\frac{dn_2}{dt}\right)^{(0)} = -\int\int\int F_1^{(0)} F_2^{(0)} \sigma^* g d\Omega d\mathbf{c}_1 d\mathbf{c}_2 \ , \tag{25}$$

$$\left(\frac{dT_1}{dt}\right)^{(0)} = \frac{2T_1}{3n_1}\left(\int\int\int F_1^{(0)} F_2^{(0)} (y_1'^2 - y_1^2)\sigma_{12} g d\Omega d\mathbf{c}_1 d\mathbf{c}_2 + \int\int\int F_1^{(0)} F_2^{(0)} [\tfrac{3}{2} - y_1^2]\sigma^* g d\Omega d\mathbf{c}_1 d\mathbf{c}_2\right) \ , \tag{26}$$

$$\left(\frac{dT_2}{dt}\right)^{(0)} = \frac{2T_2}{3n_1}\left(\int\int\int F_1^{(0)} F_2^{(0)} (y_2'^2 - y_2^2)\sigma_{12} g d\Omega d\mathbf{c}_1 d\mathbf{c}_2 + \int\int\int F_1^{(0)} F_2^{(0)} [\tfrac{3}{2} - y_2^2]\sigma^* g d\Omega d\mathbf{c}_1 d\mathbf{c}_2\right) \ , \tag{27}$$

where $y_\gamma^2 = m_\gamma c_\gamma^2 / 2kT_\gamma$. Equations (26) and (27) include the energy exchange between components owing to elastic collisions as well as that due to reactive collisions. With the substitution of the expansion, Eq. (24), into the Boltzmann equations, Eqs. (2) and (3), we get the uncoupled set of integral equations to zero order in ϵ,

$$\int\int F_\gamma^{(0)} F^{(0)} [\phi_\gamma' + \phi' - \phi_\gamma - \phi]\sigma_{\gamma\gamma} g d\Omega d\mathbf{c} = F_\gamma^{(0)} G_\gamma(c_\gamma), \quad \gamma = 1,\ 2 \ , \tag{28}$$

where

$$G_\gamma(c_\gamma) = -\frac{1}{n_\gamma}\left(\frac{dn_\gamma}{dt}\right)^{(0)} - \frac{1}{T_\gamma}(\tfrac{3}{2} - y_\gamma^2)\left(\frac{dT_\gamma}{dt}\right)^{(0)} - \int\int [F_\gamma^{(0)'} F_\eta^{(0)'} - F_\gamma^{(0)} F_\eta^{(0)}]\sigma_{12} g d\Omega d\mathbf{c}_\eta + \int\int F_\eta^{(0)} \sigma^* g d\Omega d\mathbf{c}_\eta \ , \tag{29}$$

where $y_\gamma^2 = m_\gamma c_\gamma^2 / 2kT_\gamma$. The inhomogeneous terms, $G_\gamma(c_\gamma)$, involve the unlike elastic collision terms evaluated to lowest order. These terms vanish only when the two temperatures are equal; $T_1 = T_2$. These terms do not appear in the corresponding inhomogeneous terms, $H_\gamma(c_\gamma)$ [see Eq. (10)] in the WNE approach.

We employ the expansions

$$\phi_\gamma(y_\gamma) = \sum_{j=2}^{N} b_j^{(\gamma)} S_\gamma^{(j)}(y_\gamma^2) \tag{30}$$

in Eq. (28) and get the set of algebraic equations for the coefficients $b_j^{(\gamma)}$ given by

$$\sum_{j=2}^{N} n_1^2 [S_\gamma^{(i)}, S_\gamma^{(j)}] b_j^{(\gamma)} = n_1 n_2 \beta_i^{(\gamma)}, \quad \gamma = 1, 2 \ , \tag{31}$$

where the square bracket matrix elements $[S_\gamma^{(i)}, S_\gamma^{(j)}]$ are the one-component matrix elements employed in a previous paper [5]. The coefficients $\beta_i^{(\gamma)}$ depend on the two temperatures T_1 and T_2 and are defined by

$$n_1 n_2 \beta_i^{(\gamma)} = \int F_\gamma^{(0)} G_\gamma S_\gamma^{(i)} d\mathbf{c}_\gamma. \tag{32}$$

The integrals in Eq. (29) involve the lowest order matrix elements of the unlike species collision operator that were evaluated elsewhere [30]. These are discussed again in the next section. With the definition of the species densities and temperatures

$$n_\gamma = \int F_\gamma^{(0)} d\mathbf{c}_\gamma \tag{33}$$

and

$$\tfrac{3}{2} n_\gamma k T_\gamma = \tfrac{1}{2} \int F_\gamma^{(0)} m_\gamma c_\gamma^2 d\mathbf{c}_\gamma \tag{34}$$

we have that

$$\int F_\gamma^{(0)} \phi_\gamma d\mathbf{c}_\gamma = 0 \tag{35}$$

and

$$\int F_\gamma^{(0)} m_\gamma c_\gamma^2 \phi_\gamma d\mathbf{c}_\gamma = 0,$$

so that $b_0^{(\gamma)} = b_1^{(\gamma)} = 0$. For the SNE, the fractional decrease in the equilibrium rate of reaction is given by

$$\eta^{\mathrm{SNE}} = -\sum_{\gamma=1}^{2}\sum_{i=2}^{N} b_i^{(\gamma)} A_i^{(\gamma)}(T_1, T_2)/A_0(T_1, T_2). \tag{36}$$

The set of equations, Eq. (31), is coupled to the time-dependent equations for n_γ and T_γ, Eqs. (25)–(27). The solution of Eq. (31) requires specifying an initial condition, integrating Eqs. (25)–(27), and inverting Eq. (31) at each time. This is very similar to WNE, for which the correction η^{WNE}, Eq. (18), varies implicitly with time through $n_\gamma(t)$ and $T(t)$. However, the matrix equations (12) and (13) can be inverted for chosen values of n_γ, m_γ, and $\epsilon^* = E^*/kT$ and the variation of η^{WNE} can

be studied [5–7]. In the SNE case, the matrix equation, Eq. (31), can be inverted for a set of values n_γ, m_γ, and $\epsilon^* = E^*/kT_{\text{eff}}$, where T_{eff} represents the "effective" temperature $(m_1T_2+m_2T_1)/(m_1+m_2)$. We have chosen to set the T_γ values to those that result from the WNE solution and given by Eq. (20). In Sec. V, we show the variation of η^{SNE} versus the system parameters for this choice of T_γ.

In the work of Pascal and Brun [13], the results with the SNE do not correspond to the results with the WNE when the vibrational and translational temperatures are equal. The reason for this is that the collision operators that are inverted are not the same in the two formalisms owing to the assumptions of the model. This can be understood by comparing Eqs. (28) with Eq. (8) and (9), where in the former case, only the self-collision (1-1 and 2-2 collisions) operators are inverted, whereas in the latter case, both self-collision and unlike-collision (1-2 and 2-1 collisions) operators are inverted. For the special case where the two species are identical and $T_1 = T_2$, the WNE and SNE coincide. The two unlike-collision operators add and are equal to the self-collision operator, so that Eqs. (12) and (13) are equivalent. The number of collisions in the WNE is thus twice the number of collisions in the SNE because in the former case one effectively counts the number of self-collisions twice [6].

IV. MODIFIED STRONG NONEQUILIBRIUM (MSNE)

Pascal and Brun [13] introduced a modification to SNE in order that the results would agree with the WNE results in the limit $T_{\text{vib}} = T_{\text{trans}}$. This involves including a higher order term in the perturbative analysis of the Boltzmann equations leading to Eqs. (28). If the terms linear in ϵ are retained on the LHS of the Boltzmann equations, Eqs. (22) and (23), then in place of Eq. (28) we get

$$\int\int F_1^{(0)}F^{(0)}[\phi_1'+\phi'-\phi_1-\phi]\sigma_{11}gd\Omega d\mathbf{c}+\int\int[F_1^{(0)'}F_2^{(0)'}\phi_1'-F_1^{(0)}F_2^{(0)}\phi_1]\sigma_{12}gd\Omega d\mathbf{c}$$
$$+\int\int[F_1^{(0)}F_2^{(0)}\phi_2'-F_1^{(0)'}F_2^{(0)'}\phi_2]\sigma_{12}gd\Omega d\mathbf{c}_2=F_1^{(0)}G_1(c_1)\ , \quad (37)$$

$$\int\int f_2^{(0)}f^{(0)}[\phi_1'+\phi'-\phi_1-\phi]\sigma_{22}gd\Omega d\mathbf{c}+\int\int[F_1^{(0)'}F_2^{(0)'}\phi_2'-F_1^{(0)}F_2^{(0)}\phi_2]\sigma_{12}gd\Omega d\mathbf{c}_1$$
$$+\int\int[F_1^{(0)'}F_2^{(0)'}\phi_1'-F_1^{(0)}-F_2^{(0)}\phi_1]\sigma_{12}gd\Omega d\mathbf{c}_1=F_2^{(0)}G_2(c_2) \quad (38)$$

analogous to Eqs. (8) and (9) in WNE but with the important distinction that $F_1^{(0)'}F_2^{(0)'} \neq F_1^{(0)}F_2^{(0)}$ because the species temperatures differ. The inhomogeneous terms are as defined by Eqs. (29) in the SNE approach. The unlike species collision operators on the LHS of Eqs. (37) and (38) are not self-adjoint in contrast to the situation for WNE. This aspect of this approach has been discussed at length by Pascal and Brun following the original work by Kogan *et al.* [21] and Alexeev *et al.* [22]. An important consideration is that the solution of the homogeneous equation with the adjoint collision operators, corresponding to Eqs. (37) and (38), must be orthogonal to the inhomogeneous terms $F_\gamma^{(0)}G_\gamma$ in order for unique solutions to exist [13,14]. Consequently, it has been assumed [13,21,22] that one can neglect the non-self-adjoint part of the collision operators in Eqs. (37) and (38). We adopt this procedure in the present paper and provide the justification later in connection with specific applications.

With the expansion

$$\psi_\gamma(x_\gamma)=\sum_{i=2}^{N}c_j^{(\gamma)}S_\gamma^{(j)}(x_\gamma^2) \quad (39)$$

in Eqs. (37) and (38), we get the set of algebraic equations for the coefficients $c_j^{(\gamma)}$ given by

$$\sum_{j=2}^{N}\left[\left(n_1^2[S_1^{(i)},S_1^{(j)}]+n_1n_2\langle S_1^{(i)},S_1^{(j)}\rangle^S\right)c_j^{(1)}\right.$$
$$\left.+n_1n_2\langle S_1^{(i)},S_2^{(j)}\rangle^S c_j^{(2)}\right]=n_1n_2\beta_i^{(1)}, \quad (40)$$

and

$$\sum_{j=2}^{N}\left[\left(n_2^2[S_2^{(i)},S_2^{(j)}]+n_1n_2\langle S_2^{(i)},S_2^{(j)}\rangle^S\right)c_j^{(2)}\right.$$
$$\left.+n_1n_2\langle S_2^{(i)},S_1^{(j)}\rangle^S c_j^{(1)}\right]=n_1n_2\beta_i^{(2)}. \quad (41)$$

The angular bracket matrix elements $\langle S_\gamma^{(i)},S_\eta^{(j)}\rangle^S$ are the self-adjoint part of $\langle S_\gamma^{(i)},S_\eta^{(j)}\rangle$ and depend on the two temperatures T_1 and T_2. The non-self-adjoint part of these matrix elements vanishes for $T_1 = T_2$. If the difference between the temperatures is small, then the neglect of the non-self-adjoint part of the operators is justified. The expression for η^{MSNE} is identical to the expression Eq. (36).

As discussed in Sec. III, the set of equations, Eqs. (40) and (41), is coupled to the time-dependent equations for n_γ and T_γ, Eqs. (25)–(27). Their solution requires specifying an initial condition, integrating Eqs. (25)–(27) and inverting Eqs. (40) and (41) at each time. However, we avoid this time-dependent problem by using the T_γ values from the WNE calculated from Eq. (20). In the following section, we discuss a comparison of the results of the WNE, SNE, and MSNE formalisms and the choice of T_γ in SNE and WNE.

V. COMPARISON OF NONEQUILIBRIUM EFFECTS WITH WNE, SNE, AND MSNE FORMALISMS

In this section, we present and compare the results for the three methods described in Secs. II–IV for the model line of centers reactive cross section, $\sigma^*_{\rm tot} = \pi d_r^2(1 - E^*/E)$, and elastic hard-sphere cross section, $\sigma_{\gamma\eta} = d^2_{\gamma\eta}/4$. The required matrix elements of the elastic collision operators have been evaluated in previous papers for equal temperatures [5,6] and unequal temperatures [30]. The moments of reactive collision terms have also been described elsewhere [5,6].

For SNE and MSNE, the species temperatures must also be specified and we proceed as follows. Consistent with the assumption that the elastic cross section is much larger than the reactive cross section, the time scale for elastic collisions is very short relative to the time scale for reactive collisions and the species temperatures quickly attain quasistationary values. In this way, Eqs. (12) and (13), (31), and (40) and (41) are inverted for the calculation of η in the WNE, SNE, and MSNE formalisms, respectively. The results depend critically on the species temperatures used in the SNE and MSNE. The species temperatures T_1 and T_2 used in the SNE and MSNE are those obtained from the inversion of the WNE equations, Eqs. (12) and (13), and calculated with Eq. (20). The values of T_γ are then used in Eqs. (31) and Eqs. (40) and (41) for the SNE and MSNE calculations, respectively. We justify this approach in Sec. VI by integrating the system of hydrodynamic equations, Eqs. (25)–(27), demonstrating the equivalence with the solution of the Chapman-Enskog system of equations (WNE).

The nonequilibrium corrections to the reaction rate, η, are shown in Figs. 1(a)–1(d). For WNE, there is only one temperature, T, the system temperature, and

$$\eta^{\rm WNE}(T) = [k(T) - k^{(0)}(T)]/k^{(0)}(T)$$

and the reduced reactive activation energy is $\epsilon^* = E^*/kT$. In the case of SNE and MSNE, the species temperatures T_1 and T_2, are used to obtain $\eta(T_1, T_2)$ defined as the fractional change from $k^{(0)}(T)$ given by

$$\eta(T_1, T_2) = [k(T_1, T_2) - k^{(0)}(T)]/k^{(0)}(T), \qquad (42)$$

where $T = [n_1T_1 + n_2T_2]/(n_1 + n_2)$. Note that the fractional decrease in the reaction rate coefficient, Eq. (42), is expressed *relative to the one-temperature system equi-*

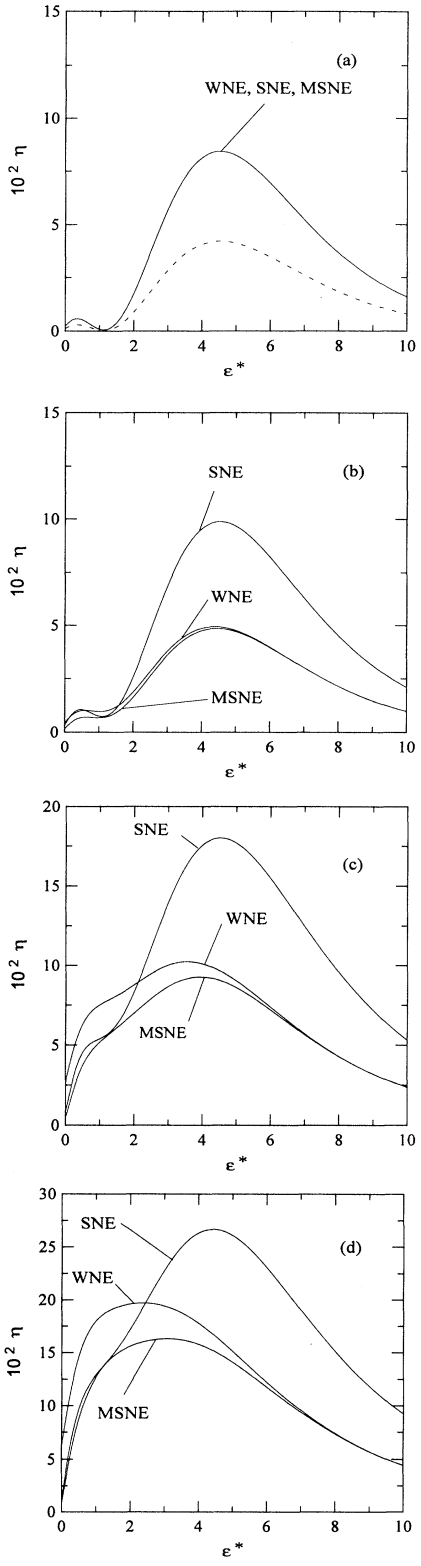

FIG. 1. Variation of η versus ϵ^* computed from the SNE, WNE, and MSNE methods for the mass ratio, m_1/m_2, equals (a) 1, (b) 1.5, (c) 3, and (d) 5. $\sigma_{11}/\sigma^* = \sigma_{22}/\sigma^* = \sigma_{12}/\sigma^* = 1$ and $n_1/n_2 = 1$. (a) shows a one component system, $A + A \rightarrow$ products (——), and a two component system, $A + B \rightarrow$ products (– – – – –).

librium rate coefficient. This serves for the purpose of comparison with the WNE. Equation (42) differs from the values for η^{SNE} and η^{MNSE} in Eq. (36). Writing Eq. (42) in terms of expansion coefficients, we get

$$\eta(T_1,T_2)=\left(\frac{k^{(0)}(T_1,T_2)-A_0}{A_0}\right)-\sum_{\gamma=1}^{2}\sum_{i=2}^{N}b_i^{(\gamma)}A_i^{(\gamma)}(T_1,T_2)/A_0. \tag{43}$$

For SNE and MSNE, ϵ^* is expressed in terms of the component temperatures and is equal to E^*/kT_{eff}, where $T_{\mathrm{eff}}=(m_1T_2+m_2T_1)/(m_1+m_2)$. For all of the numerical calculations, five to seven terms were retained in expansion of the distribution functions in Sonine polynomials and provided values of η to three significant figures.

Figures 1(a)–1(d) show the variation of η versus ϵ^* for WNE, SNE, and MSNE for a set of mass ratios, m_1/m_2 with the density ratio $n_1/n_2=1$, and $\sigma_{11}/\sigma^*=\sigma_{22}/\sigma^*=\sigma_{12}/\sigma^*=1$. The η value for the WNE is calculated with Eq. (18) and for the SNE and MSNE with Eq. (43). Figure 1(a) shows the case for which $n_1/n_2=1$, and $m_1/m_2=1$, that is for $A=B$, and the reaction reduces to $A+A\rightarrow$ products. In Fig. 1(a), the corrections obtained with the WNE, SNE, and MSNE methods are all equal, and shown with the solid curve. The dashed curve in Fig. 1(a) is the result that is obtained with the WNE and MSNE for a two-component system, $A+B\rightarrow$ products, in limit $A\rightarrow B$. The solid curve in Fig. 1(a) is the result that is obtained for a one-component system, $A+A\rightarrow$ products. For WNE and MSNE in the limit $A\rightarrow B$ the 1-1 and 1-2 collisions are indistinguishable, and hence the number of collisions is twice the number of collisions for a one-component system $A+A\rightarrow$ products. This gives a value of η for the one-component system that is twice the η value for the two-component system in the limit of identical species for the WNE and MSNE methods. For the SNE method, only 1-1 collisions are included in the collision operator that is inverted, Eq. (31).

For Figs. 1(b)–1(d) the mass ratios are 1.5, 3, and 5, respectively, and we observe differences in the behavior of η obtained from WNE, SNE, and MSNE. Figure 1(b) shows the case where the masses are slightly different ($m_1/m_2=1.5$). The SNE curve shows similar behavior to the solid curve in Fig. 1(a), but the WNE and MSNE curves are closer to the dashed curve corresponding to the two-component system. As the mass ratio increases, we observe an increase in η values, especially for $\epsilon^*\lesssim 2$. This is the result of increased temperature split between T_1 and T_2 caused by the disparity between the masses of the two components. This temperature splitting increases the departure of the system from equilibrium. Figures 1(b)–1(d) show that for $\epsilon^*>2$, the SNE result does not agree with the WNE and MSNE results. At larger ϵ^* values ($\epsilon^*>4$), there is good agreement between the WNE and MSNE results, whereas the SNE result agrees with the MSNE result for small values of $\epsilon^*\sim 0$.

Figure 2 shows the change in η versus ϵ^* for a set of density ratios with $m_1/m_2=1$ and $\sigma_{11}/\sigma^*=\sigma_{22}/\sigma^*=$

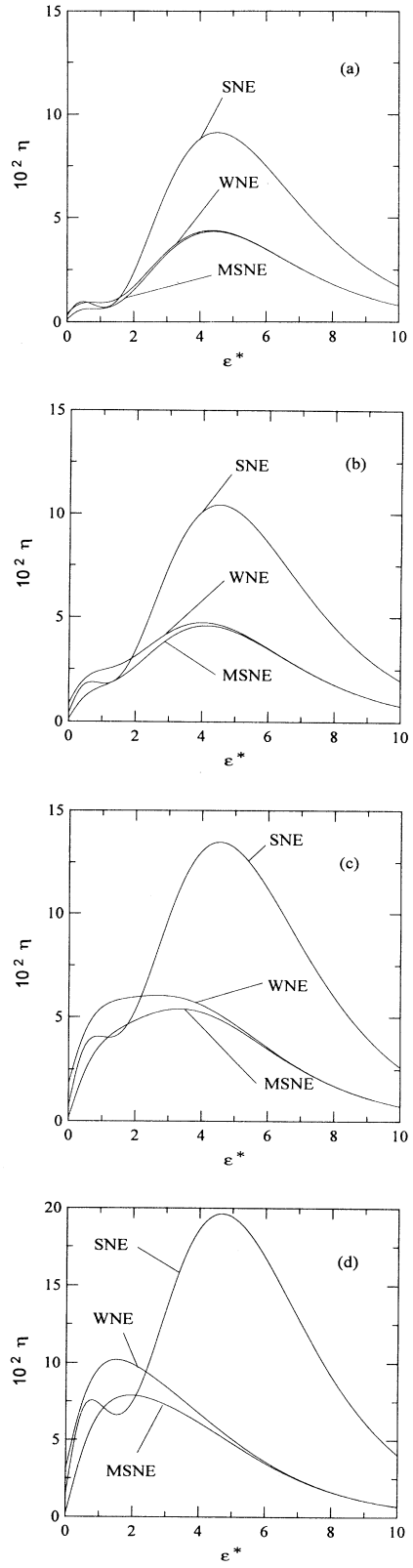

FIG. 2. Variation of η versus ϵ^* for the SNE, WNE, and MSNE methods for the reaction $A+B\rightarrow$ products for the density ratio, n_1/n_2, equals (a) 1.5, (b) 2, (c) 3, and (d) 5. $\sigma_{11}/\sigma^*=\sigma_{22}/\sigma^*=\sigma_{12}/\sigma^*=1$ and $m_1/m_2=1$.

$\sigma_{12}/\sigma^* = 1$. The density ratio between the two components, n_1/n_2 increases from 1.5 to 5 in Figs. 2(a)–2(d), respectively. As the density ratio increases, η increases. The behavior is similar to that observed by varying the mass ratios in Fig. 1. As n_1/n_2 increases from Figs. 2(a)–2(d), the difference between the two-component temperatures increases and larger η values result. The increase in η is particularly large for $\epsilon^* \lesssim 2$ due to the large influence of the different species temperatures. As the density ratio n_1/n_2 departs from unity and $\frac{m_1 n_1}{m_2 n_2}$ becomes very different from 1, we observe the effect of the larger temperature separation that results in larger η values. Again, we observe that for $\epsilon^* > 4$, the WNE and MSNE are in agreement. One notable difference between Figs. 1 and 2 is that when the density ratios become large, the SNE and MSNE do not agree for $\epsilon^* \sim 0$.

VI. TIME-DEPENDENT SPECIES TEMPERATURES; COMPARISON WITH WNE

The WNE approach involves the expansion of a distribution function about the Maxwellian at one temperature, although different species temperatures are calculated from Eq. (20) with the solution of the Chapman-Enskog equations, Eqs. (12) and (13). For the WNE, the departure of the species temperatures from the system temperatures, T, to lowest order is determined by retaining only the $a_1^{(\gamma)}$ coefficients in Eqs. (12) and (13), and also using Eq. (17). The result for component 1 is

$$\left(\frac{T-T_1}{T}\right)^{\mathrm{WNE}} = \frac{n_1}{n}\frac{1}{4M_1M_2}\left[M_2 - \frac{n_1}{n}\right](\epsilon^* + 1/2)e^{-\epsilon^*}. \tag{44}$$

The hydrodynamic equations, Eqs. (25)–(27), give the time-dependent behavior of the temperatures and densities of each component. We deduce the conditions under which the WNE method gives a good approximation of the hydrodynamic result by integrating the coupled set of differential equations, Eqs. (25)–(27), and comparing them with the results of the Chapman-Enskog solution. This provides an estimate for the range of validity of the Chapman-Enskog method. We show in Fig. 3, for different choices of the time scale parameter $\tau_E/\tau_R = \sigma^* \exp[-\epsilon^*]/\sigma_{12}$ and initial condition $T_1(0) = T_2(0)$, the results of the integration of the hydrodynamic equations, Eqs. (25)–(27). The results shown in Figs. 3(a)–3(c) are for an increasing separation in the elastic and reactive time scales. After a brief transient, the temperatures approach an asymptotic dependence which varies on a much longer time scale. We show that in the limit $\tau_E/\tau_R \to 0$ the steady solutions of Eqs. (26) and (27) coincide with WNE to the lowest order, Eq. (44). As the separation between the elastic and reactive time scales increases, the agreement between the hydrodynamic (solid curves) and the WNE results (dashed curves) improves. The ratio of elastics to reactive hard sphere collision cross-sections, $\sigma_{11}/\sigma^* = \sigma_{22}/\sigma^* = \sigma_{12}/\sigma^*$, are 1, 10, and 100 in Figs. 1(a)–1(c), respectively. The agreement improves as σ_{12}/σ^* increases, as is clear from the behavior in Fig. 3; Fig. 3(c) shows exact agreement on the reactive time scale. It is important to notice the different time and temperature scales in Figs. 3(a)–3(c) which depend on the value of σ_{11}/σ^*. The departure of T_γ from T for the two species is not equal since the density ratio $n_1/n_2 = 5$ in Fig. 3.

A comparison of the results with the WNE, that is, Eq. (44), with the long time asymptotic, quasisteady results, from the numerical integrations in Fig. 3, de-

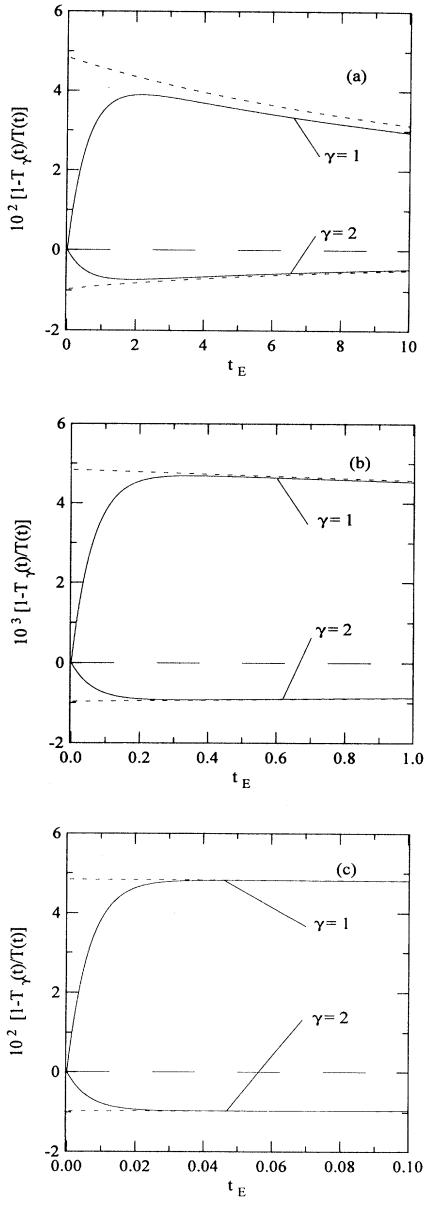

FIG. 3. Time dependence of the hydrodynamic $(1 - T_\gamma/T)$ (——), and the corresponding Chapman-Enskog values, $a_1^{(\gamma)}$ (– – – – –). The elastic collision cross sections $\sigma_{11}/\sigma^* = \sigma_{22}/\sigma^* = \sigma_{12}/\sigma^*$ are (a) 1, (b) 10, and (c) 100, with $E^*/kT(0) = 3$, $n_1(0)/n_2(0) = 5$, and $m_1/m_2 = 1$.

TABLE I. Comparison of asymptotic temperature values, $\left(\frac{T-T_1}{T}\right)^{\text{asy}}$, calculated from integration of hydrodynamic equations and corresponding one-term Chapman-Enskog values, $\left(\frac{T-T_1}{T}\right)^{\text{WNE}}$. The mass ratios for components 1 and 2, m_1/m_2, is 0.5, the density ratio $n_1/n_2 = 1.0$, and $\sigma/\sigma^* = \sigma_{11}/\sigma^* = \sigma_{22}/\sigma^* = \sigma_{12}/\sigma^*$.

E^*/kT	σ/σ^*	τ_E/τ_R [a]	$\left(\frac{T-T_1}{T}\right)^{\text{asy}}$	$\left(\frac{T-T_1}{T}\right)^{\text{WNE}}$	$\left(\frac{T-T_1}{T}\right)^{\text{asy}}/\left(\frac{T-T_1}{T}\right)^{\text{WNE}}$
1	1	3.68[-1][b]	3.355[-2]	4.484[-2]	0.748
2	1	1.35[-1]	1.919[-2]	2.529[-2]	0.759
4	1	1.83[-2]	5.529[-3]	6.502[-3]	0.851
1	100	3.68[-3]	5.129[-4]	5.157[-4]	0.995
2	100	1.35[-3]	3.125[-4]	3.140[-4]	0.995
4	100	1.83[-4]	7.651[-5]	7.668[-5]	0.995
1	1000	3.86[-4]	5.167[-5]	5.171[-5]	0.999
2	1000	1.35[-4]	3.165[-5]	3.168[-5]	0.999
4	1000	1.83[-5]	7.721[-6]	7.721[-6]	1.000

[a] $(\sigma/\sigma^*)e^{-\epsilon^*}$.
[b] $[-n] = \times 10^{-n}$ here and in following tables.

noted by $\left(\frac{T-T_1}{T}\right)^{\text{asy}}$, is shown for a range of different system parameters in Table I. As the ratio of elastic to reactive time scales becomes sufficiently large, the ratio $\left(\frac{T-T_1}{T}\right)^{\text{asy}}/\left(\frac{T-T_1}{T}\right)^{\text{WNE}}$ approaches unity. This aspect of the Chapman-Enskog approach has been discussed before [8,31,32]. The basic conclusion is that the separation of elastic and reactive time scales must be of the order of 10^{-3} to 10^{-4} for the Chapman-Enskog approach to be valid. For this situation, the departure from equilibrium will be correspondingly very small.

We have employed the WNE species temperatures to define the two-temperature matrix elements for calculating η^{SNE} and η^{MSNE} as discussed in Secs. III and IV. It is useful to mention that the study of similar nonequilibrium effects by Cukrowski and co-workers [9,10] used the solutions of the lowest order hydrodynamic equations, Eqs. (26) and (27), and an estimation of the η with the first order terms in Eq. (43).

VII. TIME-DEPENDENT SOLUTION

The Chapman-Enskog-type solutions discussed in Secs. II–IV give the long-term behavior on the reactive time scale. The solutions obtained are a special set of *normal* solutions that describe the quasistationary perturbed system. In this section we consider an explicit time-dependent solution of the Boltzmann equation that does not assume very different reactive and elastic cross sections.

We are interested in the validity of the WNE, SNE, and MSNE methods versus the four time scales given in terms of σ_{11}, σ_{22}, σ_{12}, and σ^*. If σ_{11} and σ_{22} are large it is expected that initial non-Maxwellian distributions will become Maxwellian at different temperatures on a short time scale. On a longer time scale defined by σ_{12}, the two components will equilibrate. Finally, the reactive process, considered generally as the longest time scale, perturbs the distribution function from the Maxwellian.

The time-dependent distribution function is expressed as

$$F_\gamma(x,t) = F_\gamma^{(0)}[1+\psi_\gamma(x,t)], \tag{45}$$

where the local Maxwellians, $F_\gamma^{(0)}$, vary implicitly in time, t, through the number density, $n_\gamma(t)$, and temperature, $T_\gamma(t)$, and also $\psi_\gamma(x,t)$, the time-dependent perturbation from the Maxwellian. This method is analogous to the study of temperature relaxation in binary gases [32] and the application to hot atom reactions [33].

The substitution of Eq. (45) into Eqs. (2) and (3) with $\epsilon = 1$ gives

$$\begin{aligned}\frac{dF_\gamma^{(0)}[1+\psi_\gamma]}{dt} &= \int\int [F_\gamma^{(0)'}F_\eta^{(0)'} - F_\gamma^{(0)}F_\eta^{(0)}] g\sigma_{\gamma\eta} d\Omega d\mathbf{c}_\eta - \int\int F_\gamma^{(0)'}F_\eta^{(0)'} g\sigma^* d\Omega d\mathbf{c}_\eta \\ &+ \int\int F_\gamma^{(0)}F_{\gamma'}^{(0)}[\psi'_\gamma + \psi'_{\gamma'} - \psi_\gamma - \psi_{\gamma'}] g\sigma_{\gamma\gamma'} d\Omega d\mathbf{c}_{\gamma'} \\ &+ \int\int \left[F_\gamma^{(0)'}F_\eta^{(0)'}[\psi'_\gamma + \psi'_\eta] - F_\gamma^{(0)}F_\eta^{(0)}[\psi_\gamma - \psi_\eta]\right] g\sigma_{\gamma\eta} d\Omega d\mathbf{c}_{\eta'} - \int\int F_\gamma^{(0)'}F_\eta^{(0)'}\psi_\gamma g\sigma^* d\Omega d\mathbf{c}_\eta,\end{aligned}$$

$$(\gamma,\eta) = 1,2\ . \tag{46}$$

The perturbations from the local Maxwellians are expanded in Sonine polynomials

$$\psi_\gamma(x_\gamma,t)=\sum_{i=2}^{N} b_i^{(\gamma)}(t)S^{(i)}(x_\gamma^2), \tag{47}$$

where the expansion coefficients are explicitly time dependent. The set of Boltzmann equations, Eq. (46), is thus reduced to the set of coupled equations of the form

$$\frac{1}{N_i}\frac{db_i^{(\gamma)}}{dt}=\lambda_i^{(\gamma)}+\sum_{j=2}^{N}[B_{ij}^{(\gamma)}b_j^{(\gamma)}+C_{ij}^{(\eta)}b_j^{(\eta)}],$$

$$i=2,3,\ldots,N\ , \tag{48}$$

where

$$\begin{aligned}\lambda_i^{(\gamma)}&=n_\eta\langle S_\gamma^{(i)},S_\gamma^{(0)}\rangle-\frac{1}{n_\gamma}A_i^{(\gamma)}\ ,\\ B_{ij}^{(\gamma)}&=n_\gamma[S_\gamma^{(i)},S_\gamma^{(j)}]+n_\eta\langle S_\gamma^{(i)},S_\gamma^{(j)}\rangle-D_{ij}^{(\gamma)}\\ &\quad -H_{ij1}\frac{1}{T_\gamma}\frac{dT_\gamma}{dt}-\frac{1}{n_\gamma}\frac{dn_\gamma}{dt}\delta_{ij}\ ,\\ C_{ij}^{(\eta)}&=n_\eta\langle S_\gamma^{(i)},S_\eta^{(j)}\rangle+E_{ij}^{(\eta)}\ .\end{aligned} \tag{49}$$

The angle integrals, $\langle S_\gamma^{(i)},S_\eta^{(j)}\rangle$, in Eq. (49) are the two-temperature matrix elements of the collision operators as defined in reference [30], and evaluated for the hard sphere cross section. The integrals $A_i^{(1)}$ are the moments of the equilibrium reactive collision frequencies, evaluated as in Ref. [6]. The quantities H_{ijk} are the integrals of products of three Sonine polynomials and the terms that occur in Eq. (49) arise from $dF_\gamma^{(0)}/dt$ and $dS_\gamma^{(i)}/dt$. These details of the calculation have been discussed in previous papers [30,33]. The quantities $D_{ij}^{(\gamma)}$ and $E_{ij}^{(\gamma)}$ are the matrix elements of the reactive collision operator. The matrix elements B_{ij} and C_{ij} and quantity $\lambda_i^{(\gamma)}$ are implicitly time dependent through the density, given by

$$dn_1/dt=dn_2/dt=-\left[A_0^{(1)}+\sum_{j=2}^{N}b_j^{(1)}(t)A_j^{(1)}+b_j^{(2)}(t)A_j^{(2)}\right], \tag{50}$$

and the temperature, given by

$$\begin{aligned}\frac{dT_\gamma}{dt}=-\frac{2n_\eta T_\gamma}{3}\Bigg[&\langle S_\gamma^{(1)},S_\eta^{(0)}\rangle-\frac{1}{n_\gamma^2}A_1^{(\gamma)}\\ &+\sum_{j=2}^{N}\Big([\langle S_\gamma^{(1)},S_\gamma^{(j)}\rangle-D_{j1}^{(\gamma)}]b_j^{(\gamma)}\\ &+[\langle S_\gamma^{(1)},S_\eta^{(j)}\rangle-D_{j1}^{(\eta)}]b_j^{(\eta)}\Big)\Bigg].\end{aligned} \tag{51}$$

Hence, the set of equations, Eq. (48), are linear but with nonconstant coefficients. The explicit time-dependent scheme is a rigorous solution of the Boltzmann equation

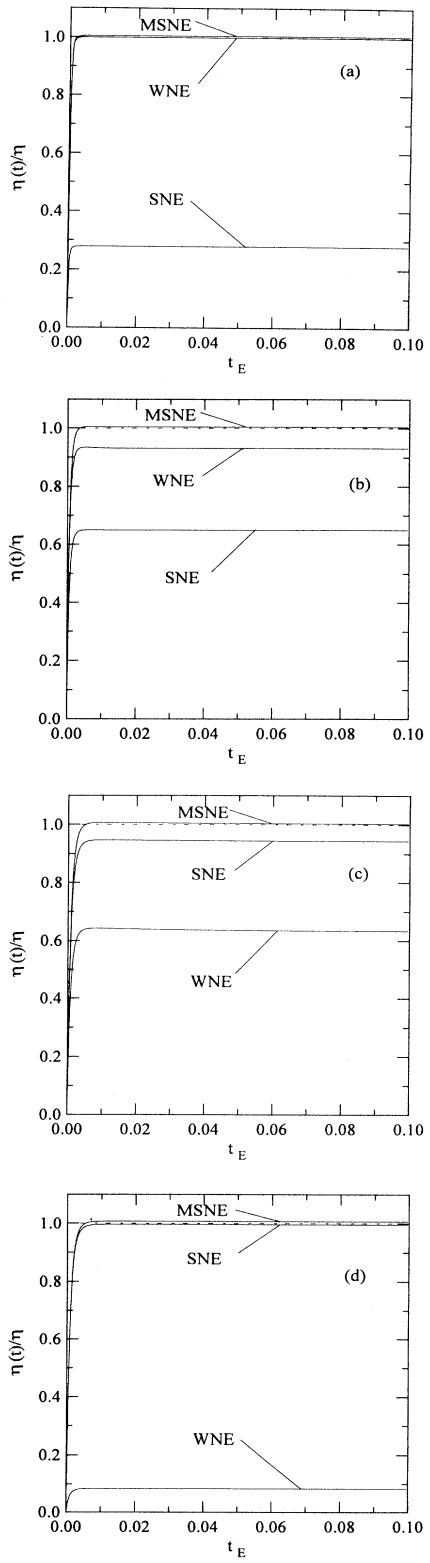

FIG. 4. Time dependence of the ratio $\eta(t)$ to η^{MSNE}, η^{WNE}, and η^{SNE} for $T_1(0)/T_2(0)=1$. The ratio of elastic to reactive hard sphere collision cross section $\sigma_{11}/\sigma^*=1000$ while σ_{12}/σ^* equals (a) 1000, (b) 200, (c) 20, and (d) 1. The ratio $\sigma_{11}/\sigma_{22}=1$, $E^*/kT(0)=10$, $m_1/m_2=3$, and $n_1(0)/n_2(0)=2$.

TABLE II. Comparison of time-dependent, WNE, SNE, and MSNE values for η for various $\sigma_{11}/\sigma^* = \sigma_{22}/\sigma^*$ and σ_{12}/σ^*. The mass ratio $m_1/m_2 = 3.0$, the initial density ratio $n_1(0)/n_2(0) = 2.0$, and $E^*/kT(0) = 10$.

Figure	σ_{11}/σ^*	σ_{12}/σ^*	$\eta^{\rm asy}$	$\eta^{\rm asy}/\eta^{\rm WNE}$	$\eta^{\rm asy}/\eta^{\rm SNE}$	$\eta^{\rm asy}/\eta^{\rm MSNE}$
4(a)	1000	1000	2.89[-5]	1.000	0.278	1.00
4(b)	1000	200	6.74[-5]	0.931	0.649	1.00
4(c)	1000	20	9.77[-5]	0.633	0.943	1.00
4(d)	1000	1	2.89[-5]	0.082	0.994	1.00

and there is no assumption about the ordering of the various terms. This scheme is used to test the validity of the WNE, SNE, and MSNE approaches.

For the numerical integration of Eqs. (48)–(51) a dimensionless time variable, t_E, is defined given by $td_e^2 n_1^{(0)}(0)/[2\pi kT_{\rm eff}(0)/m_1]^{1/2}$. The initial distribution functions are assumed to be Maxwellian [that is, $b_i^{(\gamma)}(0) = 0$] with specified initial densities, $n_\gamma(0)$. The system of coupled equations, Eqs. (48), (50), and (51), were integrated over time with a fourth-order Runge-Kutta procedure. For each time step in the numerical integration of Eqs. (48), (50), and (51), values of T_1, T_2, n_1, and n_2 were calculated and used to evaluate the matrix elements in Eqs. (12) and (13), Eq. (31), and Eqs. (40) and (41). The matrix equations were then solved and the fractional changes in the equilibrium reaction rate constant for each of the three formalisms, $\eta^{\rm WNE}$, $\eta^{\rm SNE}$, and $\eta^{\rm MSNE}$ are computed. The fractional change in the reaction rate constant at each time step was computed from $\eta(t) = -\sum_{\gamma=1}^{2}\sum_{i=2}^{N} b_i^{(\gamma)}(t)A_i^{(\gamma)}/A_0$, where the collision integrals $A_i^{(\gamma)}$ also vary with time through the species temperatures, $T_\gamma(t)$. The time-dependent solution to $\eta(t)$ eventually attains an asymptotic value, denoted by $\eta^{\rm asy}$. As for the time-independent calculations, five to seven terms were retained in the Sonine polynomial expansion of the distribution function, providing a value of η to three significant figures.

The Chapman-Enskog approach of Sec. II assumes that the reactive and elastic time scales are very well separated. This is inherent in the assumption that the time dependence is *implicit* in the time dependence of the densities and the temperature, as given by Eq. (5). This assumption has been studied in previous papers [8,31,32] and it was shown from *explicit* time-dependent calculations that the ratio of time scales should be of the order of 10^{-4} to 10^{-5} for this approach to be valid. Since the nonequilibrium effects scale as the ratio of reactive to elastic cross sections, the corrections from equilibrium obtained with the WNE method are expected to be very small.

The effect of different 1-2 time scales was studied for the time evolution of $\eta(t)/\eta$, where η is the value obtained from the WNE, SNE, and MSNE methods [Eqs. (18) and (36)]. Figures 4(a)–4(d) show the time evolution of systems with decreasing values of the 1-2 elastic collision cross section ratio, σ_{12}/σ^*. Both components are initially described by Maxwellians at the same temperature, that is, $T_1(0) = T_2(0)$, with the reduced activation energy, $E^*/kT(0) = 10$. The ratio of the elastic collision cross section to reactive collision cross section for the result in Fig. 4 has been chosen sufficiently large so that the ratio of time scales, τ_E/τ_R, is small and the Chapman-Enskog type solution of the Boltzmann equation is valid. There is a clear separation of time scales in Fig. 4 with a very fast initial transient followed by a steady asymptotic result, which can differ from unity depending on the method used. Figure 4(a) with $m_1/m_2 = 3$ and $n_1(0)/n_2(0) = 4$ shows the case for which cross sections for 1-1 and 1-2 collisions are equal, $\sigma_{11}/\sigma^* = \sigma_{22}/\sigma^* = \sigma_{12}/\sigma^* = 1000$. After the initial transient, one obtains identical results for $\eta^{\rm WNE}$ and $\eta^{\rm MSNE}$ equal to $\eta^{\rm asy}$. In Figs. 4(b), 4(c), and 4(d), the ratio σ_{11}/σ_{12} is 5, 50, and 1000, respectively. With increasing σ_{11}/σ_{12} the results with MSNE remain in agreement with $\eta^{\rm asy}$, however the WNE result does not agree when the SNE result approaches $\eta^{\rm asy}$. In Fig. 4(d), we find virtually exact agreement between $\eta^{\rm asy}$ and $\eta^{\rm SNE}$ for $\sigma_{11}/\sigma_{12} = 1000$. The results in Fig. 4 are summarized in Table II. We show that when $\sigma_{12}/\sigma^* = \sigma_{11}/\sigma^* = \sigma_{22}/\sigma^*$, the variable $\eta^{\rm asy}$ is in agreement with results obtained with WNE and MSNE. As σ_{12}/σ^* decreases, there is disagreement with the WNE result while agreement with the SNE result improves. There is uniform agreement with the MSNE result for all values of σ_{12}/σ^*. The elastic and reactive time scales in Fig. 4 and Table II differ by more than a factor of 10^{-5} and are therefore sufficiently well separated to ensure that MSNE and the time-dependent results agree as shown in Table II.

Table III illustrates the variation of $\eta^{\rm asy}$ with decreasing τ_E/τ_R with all elastic cross sections equal, analogous to the situation of Fig. 4(a). We observe that when the separation of elastic and reactive time scales is large, $\tau_E/\tau_R = 10^{-7}$, there is good agreement between $\eta^{\rm asy}$ and $\eta^{\rm WNE}$. When there is only one elastic relaxation time scale, and the reactive time scale is long, we anticipate

TABLE III. Comparison of time-dependent, WNE, and SNE values for η, where $\sigma/\sigma^* = \sigma_{11}/\sigma^* = \sigma_{22}/\sigma^* = \sigma_{12}/\sigma^*$. The mass ratio $m_1/m_2 = 3.0$ and the initial density ratio $n_1(0)/n_2(0) = 2.0$.

$E^*/kT(0)$	σ/σ^*	τ_E/τ_R	$\eta^{\rm asy}$	$\eta^{\rm asy}/\eta^{\rm WNE}$	$\eta^{\rm asy}/\eta^{\rm SNE}$
2	1	1.35[-1]	2.196[-2]	0.100	0.222
5	20	3.37[-4]	4.182[-3]	0.648	0.265
2	1000	1.35[-4]	1.600[-5]	0.748	0.283
10	1	4.54[-5]	2.283[-2]	0.767	0.220
10	200	2.67[-7]	1.441[-4]	0.991	0.278
10	1000	4.54[-8]	2.900[-5]	1.000	0.278

TABLE IV. Comparison of time-dependent, WNE, and SNE values for η for various $\sigma_{11}/\sigma^* = \sigma_{22}/\sigma^*$ and σ_{12}/σ^*. The mass ratio $m_1/m_2 = 3.0$ and the initial density ratio $n_1(0)/n_2(0) = 2.0$.

$E^*/kT(0)$	σ_{11}/σ^*	σ_{12}/σ^*	τ_{11}/τ_R [a]	$\tau_{12}/\tau_m R$ [b]	η^{asy}	η^{asy}/η^{WNE}	η^{asy}/η^{SNE}
2	200	200	6.77[-4]	6.77[-4]	1.953[-4]	0.174	0.256
10	1000	200	4.54[-8]	2.27[-7]	6.74[-5]	0.931	0.649
2	200	20	6.77[-4]	6.77[-3]	2.718[-4]	0.279	0.800
5	200	20	3.37[-5]	3.37[-5]	1.252[-3]	0.362	0.868
5	200	1	3.37[-5]	6.74[-3]	1.684[-3]	0.035	0.972
10	1000	20	4.54[-8]	2.26[-6]	2.897[-5]	0.082	0.994
10	200	1	2.27[-7]	4.54[-5]	5.167[-4]	0.311	0.996
10	10000	1	4.54[-8]	4.54[-5]	1.053[-5]	0.001	0.999

[a] $(\sigma_{11}/\sigma^*)e^{-\epsilon^*}$.
[b] $(\sigma_{12}/\sigma^*)e^{-\epsilon^*}$.

that the WNE result will become valid whereas the SNE result is inapplicable. This behavior is verified in Table III. We show that η^{asy}/η^{WNE} approaches unity with decreasing τ_E/τ_R, whereas η^{asy}/η^{SNE} remains significantly less than 1.

If on the other hand, $\sigma_{11} = \sigma_{22} \neq \sigma_{12}$ and we have two elastic time scales which differ from the reactive time scale, we expect the WNE results to be inappropriate and the SNE results to be correct. This behavior is illustrated in Table IV, where τ_{11}/τ_R and τ_{12}/τ_R are varied by changing the values of $E^*/kT(0)$, σ_{11}, and σ_{22} appropriately. In Table IV, with $E^*/kT(0) = 10$ and $\sigma_{11}/\sigma^* = 1000$ and $\sigma_{12}/\sigma^* = 200$, $\eta^{asy}/\eta^{WNE} = 0.931$, whereas for $\sigma_{11}/\sigma^* = 1000$ and $\sigma_{12}/\sigma^* = 20$, $\eta^{asy}/\eta^{WNE} = 0.082$. When the separation of the time scales for 1-1 and 1-2 elastic collisions increases with σ_{11}/σ_{12} becoming large, the ratio η^{asy}/η^{SNE} is close to unity. In Table IV, where $\sigma_{11}/\sigma^* = 1000$ and $\sigma_{12}/\sigma^* = 1$, $\eta^{asy}/\eta^{SNE} = 0.999$. Note that the η^{asy} and η^{SNE} values are close only when the time scales elastic and reactive collisions are sufficiently well separated and the ratio of elastic time scales, τ_{11}/τ_{12}, is of the order of 10^{-3}.

Table V compares η^{asy} and η^{MSNE} over a series of different time scales for 1-1 elastic, 1-2 elastic, and reactive collisions. Table V shows disagreement between η^{asy} and η^{MSNE} when $E^*/kT(0) = 2$ and $\sigma_{11}/\sigma^* = 1$ and $\sigma_{12}/\sigma^* = 1$. In this case, the separation of collision time scales for elastic and reactive processes is small, with $\tau_{11}/\tau_R = \tau_{12}/\tau_R = 0.135$, and $\eta^{asy}/\eta^{MSNE} = 0.686$. We show in Table V that the ratio η^{asy}/η^{MSNE} approaches unity when the reactive time scale is long compared to the 1-1 and 1-2 elastic time scales. Table V shows that η^{asy} and η^{MSNE} agree when both 1-1 and 1-2 elastic collisions and the reactive collision time scales are well separated. The MSNE result agrees with the time-dependent result over a range of σ_{11}/σ^* and σ_{12}/σ^* values. The MSNE method is accurate so long as the elastic and reactive time scales are well separated, and in contrast to the WNE and SNE method, its applicability is not dependent on the relative length of the 1-1 collision and 1-2 collision time scales.

It is interesting to note that the initial transient behavior in Fig. 4, which occurs on the elastic time scale, is not strongly affected by the change in the 1-1 elastic and 1-2 elastic collision time scales. Figures 4(a)–4(d) evolve on the same general time scale, with a sharp rise in η on the elastic collisional time scale due to the perturbation from the chemical reaction followed by a slow relaxation on the reactive time scale. In order to observe a pronounced effect due to changing the 1-2 collisional time scale, we

TABLE V. Comparison of time-dependent and MSNE values for η for various $\sigma_{11}/\sigma^* = \sigma_{22}/\sigma^*$ and σ_{12}/σ^*. The mass ratio $m_1/m_2 = 3.0$ and the initial density ratio $n_1(0)/n_2(0) = 2.0$.

$E^*/kT(0)$	σ_{11}/σ^*	σ_{12}/σ^*	τ_{11}/τ_R [a]	τ_{11}/τ_R [b]	η^{asy}	η^{asy}/η^{MSNE}
2	1	1	1.35[-1]	1.35[-1]	2.196[-2]	0.686
2	1000	1000	1.35[-4]	1.35[-4]	1.600[-5]	0.834
2	200	200	6.77[-4]	6.77[-4]	1.953[-4]	0.891
5	20	20	3.37[-4]	3.37[-4]	4.182[-3]	0.946
2	200	20	6.77[-4]	6.77[-3]	2.718[-4]	0.971
5	200	20	3.37[-5]	3.37[-4]	1.252[-3]	0.980
5	200	1	3.37[-5]	6.74[-3]	1.684[-3]	0.986
10	200	200	2.27[-7]	2.27[-7]	1.441[-4]	0.997
10	1000	20	4.54[-8]	2.26[-6]	2.897[-5]	1.000
10	1000	1000	4.54[-8]	4.54[-8]	2.900[-5]	1.000
10	10000	1	4.54[-9]	4.54[-5]	1.053[-5]	1.000

[a] $(\sigma_{11}/\sigma^*)e^{-\epsilon^*}$.
[b] $(\sigma_{12}/\sigma^*)e^{-\epsilon^*}$.

examine a system in which the two component temperatures are initially different, that is, $T_1(0) \neq T_2(0)$. The resulting temperature equilibration perturbs the distribution function from the Maxwellian in addition to the reaction. Temperature relaxation in the absence of a reaction has been studied previously [31,32].

Figure 5 shows the time evolution of systems with parameters identical to to Fig. 4, except the initial temperature condition, $T_1(0)/T_2(0)$, is 1.5. The rate of temperature relaxation between the two components is governed by the 1-2 collision cross section. The temperature perturbation results in an overshoot of $\eta(t)/\eta$ above unity followed by relaxation to the steady result, which is close to the MSNE result in all cases. The 1-2 elastic collision parameter, σ_{12}/σ^*, is 1000, 200, 20, and 1 in Figs. 5(a)–5(d), respectively, with $\sigma_{11}/\sigma^* = 1000$. The time scales and the magnitudes of the overshoot for Figs. 4(a)–4(d) are different and are determined by the 1-2 elastic collision cross section. The sharp initial slopes that give rise to the large overshoots in Figs. 5(a)–5(c) arise from large values of the collision matrix elements, $\langle S_\gamma^{(i)}, S_\eta^{(j)} \rangle$, of Eqs. (47)–(51). The collision matrix elements are large in magnitude when the species temperatures are significantly different and the 1-2 collision cross section, σ_{12}, is large relative to the reactive cross section. Physically, this represents rapid temperature relaxation driven by collisions between particles of two components at very different temperatures. Agreement between the asymptotic steady state and the three nonequilibrium methods appears to be similar to the comparisons shown in Table II and Fig. 4. We observe agreement between values of η^{asy} and η^{WNE} when $\sigma_{11}/\sigma_{12} = 1$ [Fig. 5(a)] and disagreement when σ_{11}/σ_{12} is large [Fig. 5(d)]. Figures 5(b), 5(c), and 5(d) show the time evolution of $\eta(t)$, η^{WNE}, η^{SNE}, and η^{MSNE} where σ_{11}/σ_{12} is 5, 50, and 1000, respectively. The steady state values of $\eta(t)$ show progressively poorer agreement with η^{WNE} in Figs. 5(a)–5(d). In contrast, the values for $\eta(t)$ in the steady state are closer to η^{SNE} when $\sigma_{11}/\sigma_{12} \gg 1$. The value of η^{SNE} disagrees with that for η^{asy} in Fig. 5(a) and agreement between η^{asy} and η^{SNE} improves when $\sigma_{11}/\sigma_{12} = 1000$ in Fig. 5(d). Figures 5(a)–5(d), also show the ratio $\eta^{\text{asy}}/\eta^{\text{MSNE}}$ is very close to unity. This is because the elastic and reactive time scales are sufficiently well separated to ensure that MSNE and the time-dependent results agree as in Table II.

VIII. SUMMARY OF RESULTS

The perturbation of the distribution function from Maxwellians for reacting species of the reaction $A + B \rightarrow$ products has been studied. For elastic collisions, a hard sphere elastic collision cross section was used while a line-of-centers reactive cross section with activation energy ϵ^* was used as a model for reactive cross sections. The perturbation to the distribution function was computed using three formalisms, the WNE, SNE, and MSNE methods. These three formalisms are based on Chapman-Enskog type solutions of the Boltzmann equation. The WNE method assumes the distribution func-

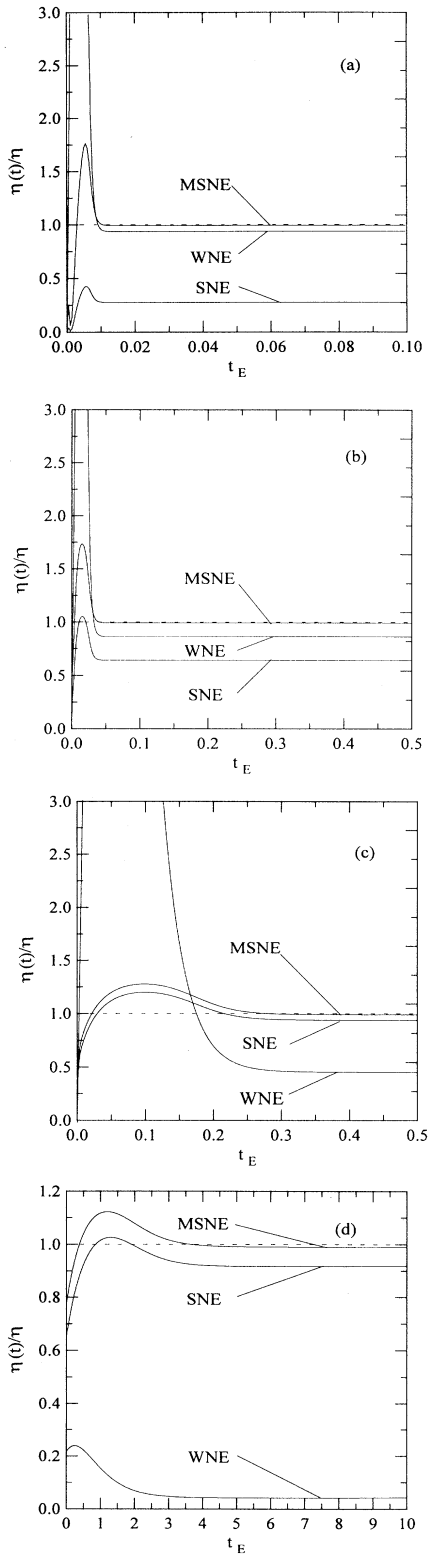

FIG. 5. Time dependence of the ratio $\eta(t)$ to η^{MSNE}, η^{WNE}, and η^{MSNE} for $T_1(0)/T_2(0) = \frac{3}{2}$. The ratio of elastic to reactive hard sphere collision cross sections is 1000 for σ_{11}/σ^* and σ_{12}/σ^* equals (a) 1000, (b) 200, (c) 20, and (d) 1. The ratio $\sigma_{11}/\sigma_{22} = 1$, $E^*/kT(0) = 10$, $m_1/m_2 = 3$, and $n_1(0)/n_2(0) = 2$.

tions of all species are characterized by one system temperature while the SNE and MSNE methods specify a temperature for each species of the system.

Unlike the system studied by Pascal and Brun [13], WNE and SNE agree in the limit in which the distribution functions of all components are characterized by perturbed Maxwellians at the same temperature. The results of WNE, SNE, and MSNE methods do not, in general, agree and an explicitly time-dependent solution of the Boltzmann equation was used to validate the solutions obtained by the three methods. The time-dependent method makes no assumptions about the ordering of the terms of the perturbation expansion of the Maxwellian and is considered a reliable check of the solutions produced by the WNE, SNE, and MSNE methods. We showed that the WNE method is appropriate for systems characterized by two time scales, the elastic and reactive time scales, when both differ by a factor of greater than 10^{-5}. The SNE method is accurate when there are three distinct time scales, and the 1-1 or self-collision, the 1-2 or non-self-collision, and reactive collision time scales are all well separated. We also show that the MSNE method is more widely applicable than either of the previous two methods and is accurate when the reactive time scale is much longer that the elastic time scale. The formalisms in the present paper should find useful applications to nonequilibrium effects in spatially nonuniform systems and the study of nonlocal transport.

IX. ACKNOWLEDGMENT

This research is supported by a grant from the Natural Sciences and Engineering Research Council of Canada.

[1] I. Prigogine and E. Xhrouet, Physica **15**, 913 (1949); I. Prigogine and M. Mahieu, *ibid.* **16**, 51 (1952).
[2] R. D. Present, J. Chem. Phys. **31**, 747 (1959).
[3] J. Ross and P. Mazur, J. Chem. Phys. **35**, 19 (1961).
[4] C. W. Pyun and J. Ross, J. Chem. Phys. **44**, 1087 (1964).
[5] B. Shizgal and M. Karplus, J. Chem. Phys. **52**, 4262 (1970).
[6] B. Shizgal and M. Karplus, J. Chem. Phys. **54**, 4345 (1970).
[7] B. Shizgal and M. Karplus, J. Chem. Phys. **54**, 4257 (1970).
[8] B. Shizgal, J. Chem. Phys. **55**, 76 (1970); Chem. Phys. **5**, 29 (1974).
[9] A. S. Cukrowski, S. Fritzsche, and J. Popielawski, in *Proceedings of the International Symposium of Far-from-Equilibrium Dynamics of Chemical Systems, Swidno, Poland, 1990*, edited by J. Popielawski and J. Gorecki (World Scientific, Singapore, 1991).
[10] A. S. Cukrowski, J. Popielawski, L. Qin, and J. S. Dahler, J. Chem. Phys. **97**, 9086 (1992).
[11] G. A. Tirsky, Annu. Rev. Fluid Mech. **25**, 151 (1993).
[12] B. Shizgal and A. S. Clarke, Chem. Phys. **166**, 317 (1982); T. J. Sommerer and M. J. Kushner, J. Appl. Phys. **70**, 1240 (1991); D. L. Flamm and D. M. Manos, *Plasma Etching: An Introduction* (Academic Press, New York, 1989).
[13] S. Pascal and R. Brun, Phys. Rev. E **47**, 3251 (1993).
[14] S. Chapman and T. G. Cowling, *The Mathematical Theory of Nonuniform Gases* (Cambridge University Press, Cambridge, 1970).
[15] S. Braginski, Rev. Plasma Phys. **1**, 205 (1965).
[16] N. N. Ljepojevic and P. MacNiece, Sol. Phys. **117**, 123 (1986); Phys. Rev. A **40**, 981 (1989); J. F. Luciani and P. Mora, Phys. Rev. Lett. **62**, 2687 (1989); J. F. Luciani, P. Mora, and R. Pellet, Phys. Fluids **28**, 835 (1985).
[17] I. D. Boyd, G. Chen, and G. V. Chandler, Phys. Fluids **7**, 210 (1995).
[18] V. V. Belyi, W. Demonlin, and I. Paiva-Veretnicoff, Phys. Fluids B **1**, 305 (1989); **1**, 317 (1989).
[19] J. Barrett, L. Demio, and B. Shizgal, Phys. Rev. A **45**, 3687 (1992).
[20] J. D. Scudder, Astrophys. J. **398**, 299 (1992); **398**, 319 (1992).
[21] M. N. Kogan, V. S. Galkin, and M. F. Makashev, *Rarefied Gas Dyanamics*, edited by R. Campargue (Commissariat a l'Energie Atomique, Paris, 1979).
[22] B. V. Alexeev, I. T. Grushin, and L. P. Grushina, *Rarefied Gas Dynamics*, edited by A. E. Beylich (VCH Vertegsgesellscheft, Weinbein, 1991).
[23] B. V. Alexeev, A. Chikhaoui, and I. T. Grushin, J. Chem. Phys. **49**, 2089, 1994.
[24] B. V. Alexeev, A. Chikhaoui, J. G. Méolans, I. T. Grushin, and L. P. Grushina, Phys. Plasmas **1**, 10 (1994); **1**, 3199 (1994).
[25] A. R. Barakat and R. W. Schunk, Plasma Physics **24**, 389 (1982).
[26] H. G. Demars and R. W. Schunk, J. Phys. D **12**, 1051 (1979).
[27] A. R. Hochstim and G. A. Massel, *Kinetic Processes in Gases and Plasmas*, edited by A. R. Hochstim (Academic Press, City, 1969).
[28] L. S. L. Lin, L. A. Viehland, and E. A. Mason, Chem. Phys. **37**, 411 (1979).
[29] B. Shizgal and M. J. Lindenfeld, Chem. Phys. **41**, 81 (1979).
[30] B. Shizgal and M. J. Fitzpatrick, Chem. Phys. **6**, 54 (1974).
[31] B. Shizgal and M. J. Fitzpatrick, J. Chem. Phys. **63**, 131 (1975).
[32] B. Shizgal and M. J. Fitzpatrick, J. Chem. Phys. **63**, 138 (1975).
[33] B. Shizgal and M. J. Fitzpatrick, J. Chem. Phys. **72**, 3143 (1980).